TÜBİTAK

Turkish Journal of Botany

http://journals.tubitak.gov.tr/botany/

Research Article

Turk J Bot
(2014) 38: 1132-1146

doi:10.3906/bot-1404-38

Patterns of phylogeography and vicariance of *Chamaerops humilis* L. (Palmae)

Juan Luis GARCÍA-CASTAÑO[1,2,*], Anass TERRAB[1,2], María Ángeles ORTIZ[1], Tod Falor STUESSY[2], Salvador TALAVERA[1]

[1]Department of Plant Biology and Ecology, University of Seville, Seville, Spain
[2]Department of Systematic and Evolutionary Botany, Biodiversity Centre, University of Vienna, Vienna, Austria

Received: 08.04.2014 • **Accepted:** 12.08.2014 • **Published Online:** 17.11.2014 • **Printed:** 28.11.2014

Abstract: *Chamaerops humilis* L. is 1 of 2 native palms occurring in Europe and the only native palm in the West Mediterranean region. Our aims were: (1) to describe its phylogeographic structure; (2) to infer a biogeographic scenario to explain its present distribution; and (3) to assess changes in its distribution from the last interglacial period. Twenty-two populations were sampled. An amplified fragment length polymorphism analysis produced 226 fragments, which allowed recognition of 4 groups of populations: (1) E Iberian Peninsula plus Al Hoceima (NE Morocco), the Balearics, and Sardinia; (2) France, the Italian Peninsula, and Sicily; (3) SW Iberian Peninsula and NW Morocco; and (4) S Morocco (var. *argentea* André; the first 3 groups are currently included in var. *humilis*). The phylogenetic information and molecular clock-related estimates, combined with geological and fossil history from the Eocene to present, suggest that *C. humilis* occurred in Central Europe in the Tertiary, reaching (1) Spain and (2) Italy, with expansion from here across North Africa to (3) N Morocco and S Spain, and (4) S Morocco. Climatic changes may also help explain the fragmented current distribution of this species. The groups of populations are sufficiently genetically distinct to recommend conservation of at least some populations in each region.

Key words: Amplified fragment length polymorphisms, fossils, Mediterranean, palms, phylogeography, Quaternary, Tertiary

1. Introduction

Dramatic changes in the past 30 million years (Ma) in the West Mediterranean region have taken place in geology and climate, resulting in significant biogeographic impacts. The closing of the Tethys Sea, the isolation of the Mediterranean from the Atlantic Ocean, and the more recent Pleistocene glaciations are only 3 of the more prominent events that have affected plant distributions in this region (Thompson, 2005). It is not surprising, therefore, that a number of investigations have attempted to understand better the biogeographic and evolutionary implications in different species within this dynamic region (Ortiz et al., 2009).

One of the most precise means of revealing the biogeographic history of plants within any region is the use of molecular markers at the population level. The spatial distribution of alleles for which phylogenetic relationships can be estimated is referred to as phylogeography (Avise, 2000). Markers often employed in these studies are haplotypes from the chloroplast genome as well as microsatellites (plastid and/or nuclear) and amplified fragment length polymorphisms (AFLPs).

A number of studies have investigated phylogeographic patterns and processes in the West Mediterranean region. They have focused primarily on relationships established during the Tertiary in genera such as *Erophaca* (Casimiro-Soriguer et al., 2010), or *Quercus* and *Pinus* (Magri et al., 2007). Several studies have also examined environmental impacts and population changes during and after the Pleistocene, such as in *Abies* (Terrab et al., 2007), *Hypochaeris* (Ortiz et al., 2009), or *Juniperus* (Terrab et al., 2008).

Another genus worth investigating, due to its interesting Euro-African distribution and rich fossil record, is *Chamaerops* L. (Palmae). This genus contains only a single species, *Chamaerops humilis* L., native to the West Mediterranean (Figure S1, online). It is 1 of 2 palms native to Europe and it is also the palm that occurs at the most northern latitudes (del Cañizo, 2011). This palm species was also reported during classical times (Gaius Plinius Secundus, better known as Pliny the Elder, 1st century AD), suggesting possible ancient traditional human use.

Chamaerops belongs to tribe Trachycarpeae of subfamily Coryphoideae (Dransfield et al., 2008), and

* Correspondence: jlgc@us.es

molecular phylogenetic studies reveal that the closest generic relatives are *Guihaia* J.Dransf., S.K.Lee & F.N.Wei; *Trachycarpus* H.Wendl.; *Rhapidophyllum* H.Wendl. & Drude; *Maxburretia* Furtado; and *Rhapis* L.f. ex Aiton (Baker et al., 2009). It is small, multistemmed, and rhizomatous, with palmate leaves (do Amaral Franco, 1980; Herrera, 1989; del Cañizo, 2011) and of variable life form, leaf colour, and presence of thorns (Maire, 1980). The reproductive system of this dioecious species is interesting; it has leaf-mediated pollination, whereby the leaves release scents attractive to coleopterans (Herrera, 1989; Düfay and Anstett, 2004), and it has mammal-mediated dispersal of its fleshy fruits, mainly by foxes or badgers (Fedriani and Delibes, 2011).

The present distribution of *C. humilis* is restricted to the West Mediterranean (Médail and Quézel, 1996), both on the European (where it is the only native palm species) and African sides (Figure 1). In Europe, it occurs on the coasts of S Portugal, S and E Spain, SE France (rediscovered by Médail and Quézel, 1996), and W Italy. In Africa, it occurs mainly in Morocco but also in N Algeria and N Tunisia. In Libya it apparently has become extinct (Jafri and El-Gadi, 1977). The species has its widest distribution in Morocco, where 2 varieties have been distinguished: a form with green leaves in the north (var. *humilis*) and a form with glaucous leaves in the south (var. *argentea* André), which is often found at very high altitudes of up to 2000 m (Maire, 1980; Govaerts and Dransfield, 2005). The species also occurs on most of the large islands of the West Mediterranean, i.e. the Balearics, Sardinia, Sicily, and Malta (where it apparently has become extinct). In Corsica it does not seem to be autochthonous (do Amaral Franco, 1980).

The oldest fossil records of *Chamaerops* are from the Eocene in Europe (Palamarev, 1989) and it may be considered as one of the most ancient fleshy-fruited species in the Mediterranean basin (Palamarev, 1989; Herrera, 1995). It appears, therefore, to have reduced its distribution from paratropical Eocene forests. Nowadays, with other species such as *Laurus nobilis*, it constitutes the Mediterranean '*Laurocerasus*-belt', which is surrounded by species derived from more recent geological periods (Mai, 1989).

The purposes of this paper, therefore, are: (1) to describe the phylogeographic structure of the species throughout its distributional range in the West Mediterranean region; (2) to infer a biogeographic scenario to explain its present distribution; and (3) to assess the most recent changes in the distribution of this species from the last interglacial period by use of niche modelling analyses.

2. Materials and methods

2.1. Amplified fragment length polymorphism

2.1.1. Sampling

The 22 sampled populations are shown in Figure 1 and listed in Table 1; they cover most of the distributional area of the

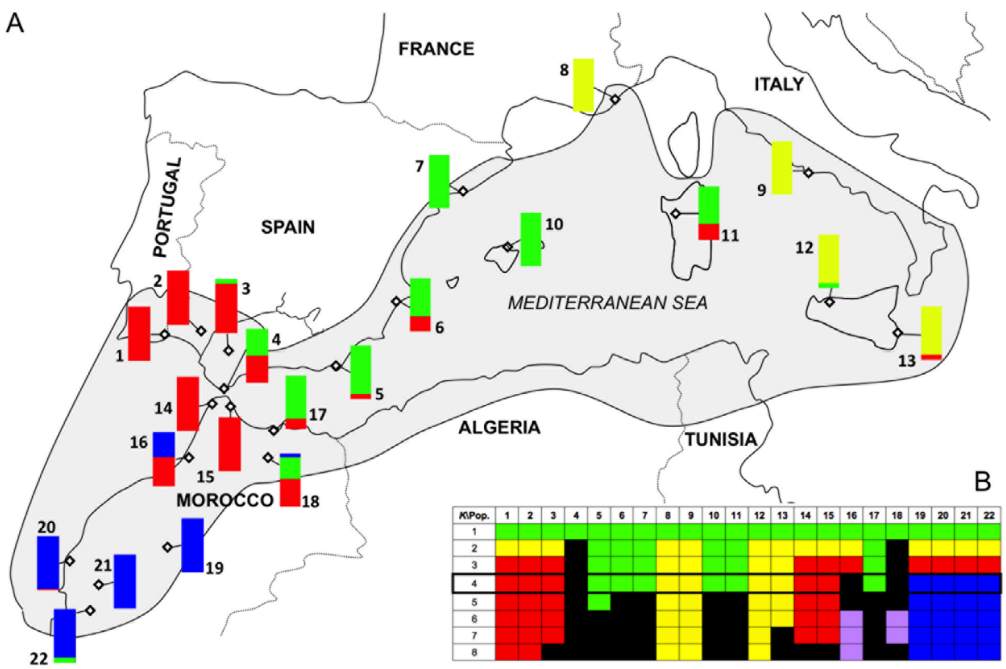

Figure 1. (A) Distribution map of *Chamaerops humilis*, populations selected for sampling and Structure results, and **(B)** colour-coded population assignment for the different Bayesian-inferred groups obtained for the different *K*s set (black colour for not clearly assignable populations, NAPs; optimal value of $K = 4$, according to the Akaike and Schwarz criteria, is highlighted); see Section 2 and Tables 1 and 2.

Table 1. Population samples of *Chamaerops humilis* and *Trachycarpus fortunei*. Origin (population, country, locality/region, and coordinates), sample size (n), $Frag_{tot}$, $Frag_{poly}$ (%), number of phenotypes (n_{ph}), H_D (mean and SE), and *DW* are shown.

Population	Country	Locality/region	Coordinates (m a.s.l.)	n	$Frag_{tot}$	$Frag_{poly}$ (%)	n_{ph}	H_D (SE)	*DW*
Continental Europe									
Portugal									
1	Portugal	Vila Real de Santo António (Algarve)	37°14′20.5″N, 7°26′16.0″W (2 m)	10	156	114 (72.1%)	10	0.272 (0.015)	268.8
Spain									
2	Spain	Hinojos (Huelva)	37°17′04.0″N, 6°23′56.0″W (55 m)	10	161	98 (60.9%)	10	0.227 (0.014)	183.9
3	Spain	Pruna (Seville)	36°59′47.1″N, 5°12′33.3″W (698 m)	10	162	105 (64.8%)	10	0.254 (0.014)	296.4
4	Spain	Tarifa (Cádiz)	36°03′23.8″N, 5°32′55.6″W (319 m)	10	162	131 (80.9%)	10	0.296 (0.015)	233.9
5	Spain	Cabo de Gata (Almería)	36°43′45.4″N, 2°11′25.4″W (27 m)	10	141	100 (70.9%)	10	0.249 (0.015)	177.3
6	Spain	Peñón de Ifach (Alicante)	38°38′20.7″N, 0°04′27.2″E (17 m)	10	156	113 (72.4%)	10	0.265 (0.015)	187.0
7	Spain	Garraf (Barcelona)	41°15′13.3″N, 1°48′57.6″E (40 m)	10	153	106 (69.3%)	10	0.252 (0.015)	193.9
France									
8	France	Cap Taillat	43°10′13.1″N, 6°38′38.3″E (36 m)	10	158	98 (62.0%)	10	0.237 (0.015)	188.5
Italy									
9	Italy	Circeo (Lazio)	41°13′54.6″N, 13°02′28.3″E (10 m)	10	155	88 (56.8%)	10	0.209 (0.015)	363.1
Mediterranean islands									
10	Spain	Cabo Formentor (Mallorca, the Balearics)	39°56′39.2″N, 3°10′16.0″E (114 m)	10	153	95 (62.1%)	7	0.224 (0.015)	253.8
11	Italy	Castelsardo (Sardinia)	40°53′29.8″N, 8°39′15.6″E (78 m)	10	159	112 (70.4%)	10	0.258 (0.015)	221.6
12	Italy	Palermo (N Sicily)	38°12′05.6″N, 13°16′03.9″E (17 m)	10	157	95 (60.5%)	10	0.237 (0.015)	303.5
13	Italy	Syracuse (S Sicily)	36°59′59.6″N, 15°15′58.0″E (9 m)	10	156	95 (60.1%)	10	0.217 (0.014)	250.0
NW Africa									
14	Morocco	Cape Spartel	35°47′22.6″N, 5°53′33.4″W (223 m)	10	165	97 (58.8%)	10	0.238 (0.015)	242.3
15	Morocco	Oued-Lau (Tétouan)	35°31′51.2″N, 5°11′55.1″W (37 m)	10	161	103 (64.0%)	10	0.246 (0.014)	238.9
16	Morocco	Sidi Yahya du Rharb (the Mamora)	34°12′14.9″N, 6°16′58.0″W (100 m)	10	159	96 (60.4%)	7	0.229 (0.014)	251.0
17	Morocco	Al Hoceima	35°13′16.1″N, 3°58′54.1″W (330 m)	10	163	117 (71.8%)	9	0.269 (0.014)	206.3
18	Morocco	Tazzeka	34°09′11.9″N, 4°18′36.8″W (367 m)	10	162	126 (77.8%)	10	0.297 (0.014)	262.9
19	Morocco	Beni Mellal	32°18′49.3″N, 6°16′16.0″W (1536 m)	10	158	92 (58.2%)	9	0.217 (0.014)	238.5
20	Morocco	Essaouira	31°30′15.4″N, 9°41′43.6″W (100 m)	10	162	102 (63.0%)	9	0.247 (0.015)	250.3
21	Morocco	Tizi-n-Test	30°48′09.2″N, 8°23′33.6″W (1110 m)	10	157	105 (66.9%)	9	0.229 (0.015)	237.6
22	Morocco	Tafraoute	29°45′24.6″N, 8°50′03.3″W (1610 m)	10	149	96 (64.4%)	10	0.236 (0.014)	217.8
TOTAL	*Chamaerops humilis* L.			220	208	201 (96.7%)	210		
Trachycarpus fortunei (Hook.) H.Wendl.	Garden	Alamillo Park nursery (Seville, Spain)	37°25′22.1″N, 5°59′40.0″W (8 m)	10	106	61 (57.5%)	8		

species, including the largest islands. In every population we collected leaf material from 10 different stems that were placed far enough apart to avoid resampling the same genetic individual; the species is rhizomatous, which required caution and care in making the field collection. Material was dried and preserved in silica gel and stored prior to DNA extraction. Vouchers of sampled populations have been deposited in the herbarium of the University of Seville (SEV). *Trachycarpus fortunei* (Hook.) H.Wendl., a species belonging to the sister clade (Baker et al., 2009), was chosen as the outgroup representative (10 individuals were analysed as well).

2.1.2. DNA extraction and AFLP protocol

Genomic DNA was extracted according to Doyle and Doyle (1987) following the CTAB protocol: after precipitation with isopropanol and centrifugation, the DNA pellet was washed with 70% ethanol and subsequently dried in a vacuum centrifuge. Finally, DNA was resuspended in TE buffer and treated with RNAse at 37 °C for 30 min.

The AFLP procedure followed established protocols (Vos et al., 1995; Blears et al., 1998). Genomic DNA (~0.5 µg) was digested with 2 restriction endonucleases, *Eco*RI and *Mse*I, and the resulting fragments were ligated to double-stranded *Eco*RI and *Mse*I adaptors at 37 °C for 2 h; the ligated DNA fragments were diluted with $TE_{0.1}$ buffer. Preselective and selective amplifications were performed in a thermal cycler (Gene Amp PCR System 9700, PE Applied Biosystems), and the polymerase chain reaction (PCR) protocols also followed Vos et al. (1995). The number of fragments was reduced ~16-fold (4 × 4) through the use of preselective primers based on the sequences of *Eco*RI and *Mse*I adaptors with the addition of nucleotides (*Eco*RI-A and *Mse*I-C), matching the nucleotide downstream from the restriction sites. Preselective PCR products were diluted with $TE_{0.1}$ buffer and then amplified with primers having 2 additional selective bases (3 in total), of which the first base was the same as that added in the previous amplification; this resulted in a further ~256-fold (16 × 16) reduction of the number of fragments, for ~4096-fold in total (16 × 256). Moreover, the *Eco*RI-based primers were labelled with fluorescent dyes. For the selective PCR, the following 3 primer combinations were used (selected, based on amplification effectiveness and variability, from a trial of 32): *Eco*RI (FAM)-ACT/*Mse*I-CAG, *Eco*RI (VIC)-AGG/*Mse*I-CAC, and *Eco*RI (NED)-ACC/*Mse*I-CAC. The fluorescence labelled selective amplification products were separated on an automated sequencer (3130*xl* Genetic Analyzer, Applied Biosystems|Hitachi). Raw data were aligned with internal 500 ROX size standard using ABI PRISM GeneScan 3.7 (Applied Biosystems, 1989–2000). The resulting GeneScan files were imported into Genographer ver. 1.6.0 (Benham et al., 1999) and the fragments scored using the 'thumbnail' option, which allowed comparison of each fragment signal over all samples; the result of the scoring process was exported as a presence/absence (1/0) matrix.

Genotyping and scoring errors are known to be very common in AFLP procedures and estimation of repeatability is recommended (Bonin et al., 2007). Repeatability was tested in 32 individuals (14.5%, 1–4 individuals per population) and was calculated as the ratio of the total number of mismatches (band presence vs. band absence) in the replicated individuals divided by the number of fragments found; this gave us an average value of 0.1 for the whole data set. Assuming that genotyping and scoring errors were randomly distributed and no bias at the population level would occur, we could follow the recommendation of 0.1-limit error (Bonin et al., 2007). Other authors such as Skrede et al. (2006) have also followed this criterion as being more than adequate to assess population-level variation.

2.1.3. Genetic diversity and population structure

Within-population genetic diversity was assessed as the total number of AFLP fragments ($Frag_{tot}$), the number and percentage of polymorphic fragments [$Frag_{poly}$ (%)], and the number of different AFLP phenotypes (n_{ph}), all of them corrected with the 0.1 scoring error obtained (i.e. considering as monomorphic those fragments that were present in at least 90% of the individuals and ignoring those fragments present only at a maximum of 10% at a population level). We also calculated the average gene diversity index per population ($H_D = 1 - \Sigma x_i^2$, where x_i is the population frequency of 'alleles' 1 and 0 at locus i; the average gene diversity is the resulting mean across all loci). The 'frequency-down-weighted marker values' index (DW) was calculated as the ratio of means.

These estimates were obtained using FAMD ver. 1.108β (Schlüter and Harris, 2006), Arlequin ver. 3.0.1 (Excoffier et al., 2005), and AFLPdat (Ehrich, 2006). FAMD ver. 1.108β was also used to gather individuals into population groups. Finally, the number of fragments exclusively shared between pairs of populations was assessed and also corrected with the scoring error obtained (i.e. at least present in more than 10% of the individuals of each population).

Pairwise F_{ST} values based on Euclidean distances for the between-groups comparison were obtained using FAMD ver. 1.108β. The matrix was exported to SplitsTree ver. 4.5 (Huson and Bryant, 2006) where a Neighbour-Net was constructed to establish the different relationships between sampled populations. The support for each node was calculated separately with FAMD ver. 1.108β, using 1000 bootstrap replicates based on chord distances for a neighbour-joining tree, by applying the Bayesian method to calculate null allele frequencies and with the among-population nonuniform prior assumption.

Bayesian analyses using Structure ver. 2.2 (Pritchard et al., 2000; Falush et al., 2003) were applied, setting a burn-in period of 1×10^5, and run separately with lengths of 5×10^5 MCMC (5 iterations) and 1×10^5 MCMC (10 iterations) for $K = 1–8$. As very long distances are usually not traversed by pollen (Carrión, 2002), the simpler no-admixture model was applied, starting at prior population information, under the assumption of allele frequencies in each population being correlated. Average groups were calculated with CLUMPP ver. 1.1 (Jakobsson and Rosenberg, 2007) and graphically displayed using Distruct ver. 1.1 (Rosenberg, 2004). A population was assigned to a specific group if it demonstrated at least 70% association. At this population level, the optimal K was selected according to the Akaike information criterion (*AIC*: Akaike, 1974; *AICc* and *AICu*: McQuarrie and Tsai, 1998) and the Bayesian or Schwarz information criterion (*BIC*: Schwarz, 1978). Additionally, principal coordinate analyses (PCoAs) based on Euclidean distances were applied to assess relationships among the individuals and populations (pairwise Φ_{ST} values), using FAMD ver. 1.108β.

To test for isolation-by-distance, pairwise F_{ST} values for populations were compared with their geographical distance using Mantel bilateral tests based on Spearman correlations (1000 permutations; XLSTAT ver. 2007.6, Addinsoft).

Finally, genetic differentiation among populations and different groupings were assessed by applying analyses of molecular variance (AMOVAs), based on Euclidean distances, using the F_{CT} values obtained with Arlequin ver. 3.0.1. For groups of populations, the number of private shared fragments was calculated and a bio-neighbour-joining tree was constructed with SplitsTree ver. 4.5 based on $\rho_{ST(2)}$ values, which were used to compensate for unequal sample sizes (El Mousadik and Petit, 1996); the bootstrap support for each node was calculated in the same way as explained above.

2.1.4. Dating analysis

The use of a molecular clock based on plastid (*atp*B, *mat*K, *rbc*L, *rps*16 intron, *trn*L–*trn*F) or nuclear (18S, ITS, *ms* –malate synthase gene) sequences was rejected, because identities between these sequences, previously analysed by Baker et al. (2009), were higher than 92% (normally 99%–100%) between *C. humilis* and *T. fortunei*. An attempt was made, therefore, to use a molecular clock based on AFLP data (Kropf et al., 2009). As has been pointed out by some authors (e.g., Ehrich et al., 2009), this clock is not free from analytical problems. D_{N72} genetic dissimilarity coefficient values were calculated with POPGENE ver. 1.32 (Yeh and Boyle, 1997). To check the feasibility of using this clock, we tested a range of F_{IS} values (0–1), rates (fast and slow rate alternatives, i.e. 0.027 Ma/D_{N72} and 0.517 Ma/D_{N72}), and generation time values, which were then calibrated at the Late Eocene. This period was chosen as fossil evidence showed that *Chamaerops* existed in Europe during the Tertiary, extending back as far as the Eocene. Fossils (stems, roots, seeds, leaves, or cuticles) assigned to *C. humilis* or very similar morphological species have been found from the Eocene (56–34 Ma) in Germany; the Lower Oligocene (34–28 Ma) in France; the Upper Oligocene (28–23 Ma) of Bulgaria; the Miocene (23–5.3 Ma) in Poland, Moldavia, and Romania; the Lower Miocene (23–16 Ma) in Sardinia; the Upper Miocene (11–5.3 Ma) in Greece; and the Pliocene (5.3–2.6 Ma) in Spain (Pons, 1981; Palamarev, 1989; Velitzelos and Gregor, 1990; Givulescu and Barbu, 1999; Palamarev et al., 2005; Kovar-Eder et al., 2006; Dransfield et al., 2008; Carrión, 2012; and references cited therein). To our knowledge, there are no fossil records from N Africa.

2.2. Niche modelling

Niche modelling analyses were conducted for 3 temporal climatic frames: the last interglacial period (~120,000–140,000 years BP; Otto-Bliesner et al., 2006), the last glacial maximum (~21,000 years BP; Braconnot et al., 2007), and the present (~1950–2000; Hijmans et al., 2005). Data for the last glacial maximum were obtained from 2 atmospheric models, from the Community Climate System Model (CCSM) and from the Model for Interdisciplinary Research on Climate (MIROC). Bioclimatic data were obtained from the WorldClim Global Climate Data web page (http://www.wordclim.org) and all 19 WorldClim variables were used. Soil data (FAO/IIASA/ISRIC/ISSCAS/JRC, 2012) were obtained from the Harmonized World Soil Database (http://webarchive.iiasa.ac.at/Research/LUC/External-World-soil-database/HWSD_Data/HWSD_RASTER.zip), with selection of the most precise mapping unit. Data sets were rescaled to 2.5 arc-minutes with Quantum GIS ver. 1.8.0-Lisboa in order to make comparable the different scenarios. Present location data were obtained from vouchers deposited in SEV, which included our extensive sampling; additionally, we added locations from Algeria (Royal Botanic Gardens Herbarium, Kew: K000208642, and K000208639, K000208640, K000208641, K000208643, and K000208644) obtained from the Global Biodiversity Information Facility (GBIF) data set (accessed 19 June 2013). Finally, predictive analyses, based on the whole set of variables, were performed using the maximum entropy method with the software MaxEnt (Phillips et al., 2006) and results were shown for 2 thresholds: maximum training sensitivity plus specificity logistic threshold and 10-percentile training presence logistic threshold.

3. Results

3.1. AFLP profile

A total of 226 fragments were obtained ranging from 60 to 447 bp (208 in *Chamaerops*), 4 of them being

monomorphic; 7 fragments were present in 90% of the *Chamaerops* individuals (for further details, see Table 1). For different primers the results were as follows: (1) *Eco*RI (NED)-ACC/*Mse*I-CAC, 51 fragments, 60–405 bp, 1 fragment monomorphic in *Chamaerops*; (2) *Eco*RI (VIC)-AGG/*Mse*I-CAC, 126 fragments, 63–447 bp, 4 fragments monomorphic in *Chamaerops*; (3) *Eco*RI (FAM)-ACT/*Mse*I-CAG, 49 fragments, 65–395 bp, 2 fragments monomorphic in *Chamaerops*. At the 90% level, 18 fragments were exclusive to *Trachycarpus fortunei* and 120 to *Chamaerops*. AFLPdat (after including 0.1 scoring error correction) showed the existence of 218 different phenotypes out of the 230 samples analysed, with 7–10 phenotypes per population.

3.2. Genetic diversity

The results of the estimated genetic diversity patterns are shown in Table 1. The number of total fragments varied from 141 in Cabo de Gata (Spain) to 165 in Cape Spartel (Morocco); the percentage of polymorphic fragments ranged from 56.8% in Circeo (Italy) to 80.9% in Tarifa (Spain); the average gene diversity (H_D) ranged from 0.209 in Circeo (Italy) to 0.296 in Tarifa (Spain) and 0.297 in Tazzeka (Morocco); and the rare fragments index (*DW*) varied from 177.3 in Cabo de Gata (Spain) to 363.1 in Circeo (Italy).

3.3. Population structure

The Bayesian analysis conducted with Structure, in conjunction with the Akaike and Schwarz criteria used to select the optimum number of clusters, pointed to the existence of 4 main groups (see Table 2 and Figure 1). These were defined from *K* 2 to 4 in the following order: (1) E Spain (Cabo de Gata, Peñón de Ifach, and Garraf; pops. 5, 6, and 7), the Balearics (pop. 10), Sardinia (pop. 11), and Al Hoceima (pop. 17; NE Morocco), hereafter labelled as the E Spain-Sardinia-NE Morocco group of populations; (2) France (pop. 8), continental Italy (pop. 9), and Sicily (Palermo and Syracuse; pops. 12 and 13), hereafter labelled as the France-Italy group of populations; (3) SW Iberian Peninsula (Portugal: Vila Real de Santo António; pop. 1; and Spain: Hinojos and Pruna; pops. 2 and 3), and NW Morocco (Cape Spartel and Tétouan; pops. 14 and 15), hereafter labelled as the S Spain-N Morocco group of populations; and (4) S Morocco: Beni Mellal (pop. 19), Essaouira (pop. 20), Tizi-n-Test (pop. 21), and Tafraoute (pop. 22), hereafter labelled as the S Morocco group of populations. Three populations showed an intermediate position between these main groups: Tarifa, pop. 4 (50% of groups 1 and 3), the Mamora, pop. 16 (54% of group 3 and 46% of group 4), and Tazzeka, pop. 18 (52% of group 3, 40% of group 1, and 8% of group 4), named nonassignable populations (NAPs) hereafter.

The Neighbour-Net obtained with the F_{ST} pairwise distances (Figure 2) is consistent with the grouping calculated with Bayesian analysis (Table 2 and Figure 1). Bootstrap values obtained were 91% BS (E Spain-Sardinia-NE Morocco group of populations), 98% BS (France-Italy group of populations), 60% BS (S Spain-N Morocco group of populations), and 75% BS (S Morocco group of populations). Tarifa, Tazzeka, and the Mamora populations also occupied an intermediate position among groups, as in the Bayesian analysis (Table 2; Figures 1 and 2).

In Figure 3A we present PCoA results for principal component (PCo) 1 (10.2%) and PCo 2 (5.5%) for the individuals analysed. The Mamora individuals appear at an intermediate position between the S Morocco and S Spain-N Morocco groups of populations, and those

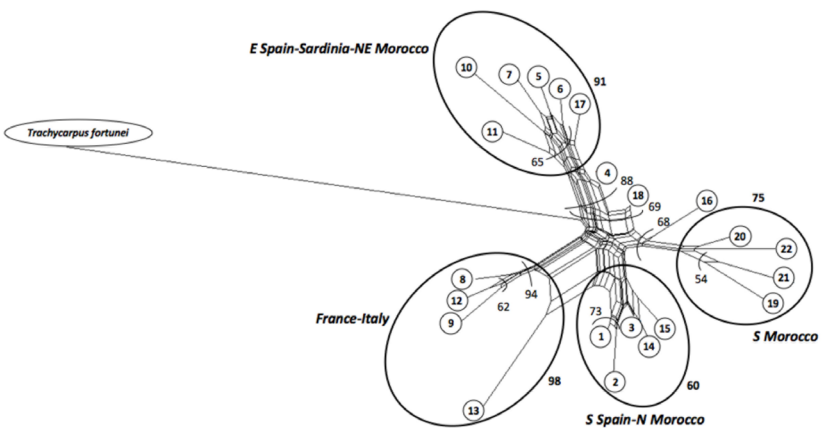

Figure 2. Neighbour-Net for the populations of *Chamaerops humilis* sampled, including *Trachycarpus fortunei* as an outgroup representative, based on the Euclidean distances. Bootstrap values obtained on the chord distances for the neighbour-joining tree; see Table 1 for codes.

Table 2. Akaike and Schwarz criteria values for the different Bayesian-inferred groups obtained for the different *K*s set (optimal value of $K = 4$ is highlighted).

K	Group SS (d.f.)	Pop. SS (d.f.)	Ind. SS (d.f.)	Total SS (d.f.)	*AIC*	*AICc*	*AICu*	*BIC*
1	0.000 (0)	2294.209 (21)	5495.000 (198)	7789.209 (219)	1409.04	4.59	4.60	784.71
2	595.009 (2)	1699.200 (19)	5495.000 (198)	7789.209 (219)	1393.56	4.52	4.53	772.62
3	937.489 (3)	1356.720 (18)	5495.000 (198)	7789.209 (219)	1384.83	4.48	4.49	767.29
4	1196.307 (4)	1097.902 (17)	5495.000 (198)	7789.209 (219)	1378.36	4.45	4.47	764.21
5	1072.849 (4)	1221.360 (17)	5495.000 (198)	7789.209 (219)	1384.44	4.48	4.50	773.68
6	1199.046 (4)	1095.164 (17)	5495.000 (198)	7789.209 (219)	1382.27	4.47	4.50	774.90
7	1068.203 (4)	1226.006 (17)	5495.000 (198)	7789.209 (219)	1388.59	4.50	4.53	784.62
8	875.551 (4)	1418.658 (17)	5495.000 (198)	7789.209 (219)	1396.81	4.53	4.58	796.23

from Tarifa and Tazzeka are dispersed in the centre of the graph. These patterns are clearer when the average values are shown (Figure 3B). If the PCoA is based on the population, not the individual, distance matrix, the percentage of variance explained is much higher (PCo 1 = 38.6% and PCo 2 = 26.9%), but the relative position of the populations remains almost the same as in Figure 3B (results not shown).

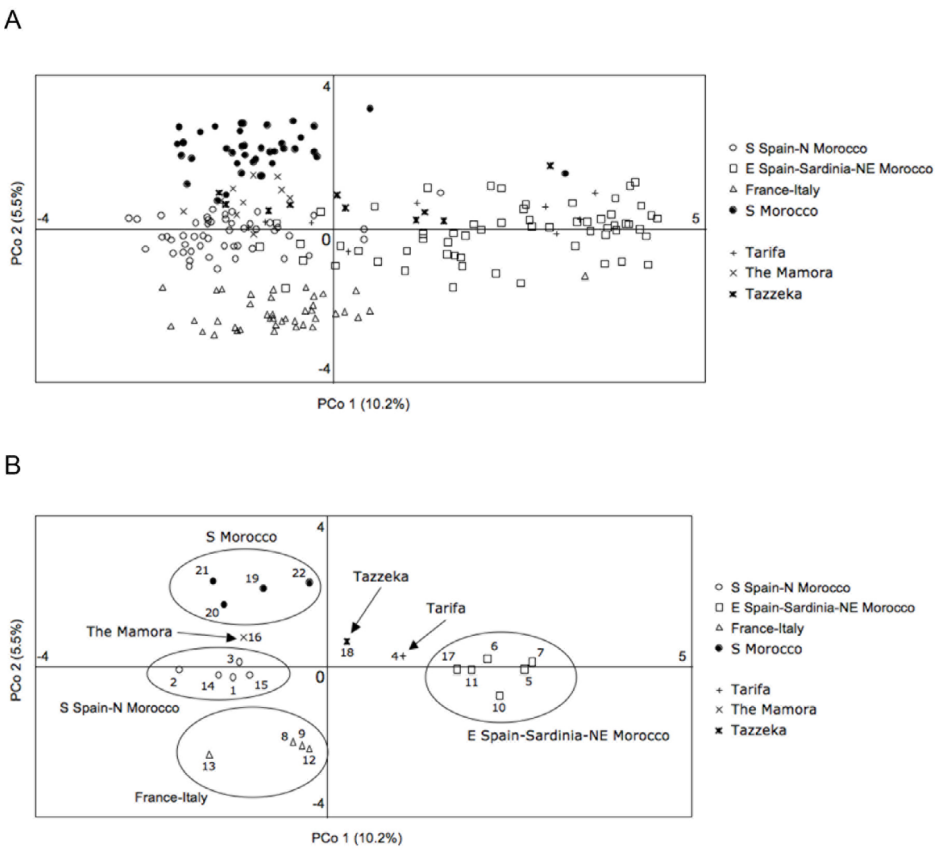

Figure 3. PCoA for the first 2 axes, showing the different Bayesian-inferred groups of populations as well as the not clearly assignable populations (NAPs) for **(A)** individuals and **(B)** their mean values per population; see Table 1 for codes.

The Mantel test applied between the geographic and the genetic distances was positively significant (Spearman's ρ = 0.629, P = 0.001). Moreover, the number of exclusive shared fragments between pairs of populations, which reveal very closely related populations, was null or very low, with only 5 matches of 1 fragment between: pop. 13 and pop. 15, 13 and 22, 18 and 21, 10 and 16, and 19 and 20.

The different AMOVAs, considering no grouping, i.e. globally, and different groupings (excluding the 3 NAPs), showed that the significantly best grouping was the same as that defined by Bayesian inference, i.e. E Spain-Sardinia-NE Morocco, France-Italy, S Spain-N Morocco, and S Morocco (Table 3).

Of the $\rho_{ST(2)}$ values calculated for the groups of population assortment, S Spain-N Morocco and S Morocco had the closest relationship ($\rho_{ST(2)}$ = 0.083), the latter showing the largest separation from France-Italy ($\rho_{ST(2)}$ = 0.128) and E Spain-Sardinia-NE Morocco ($\rho_{ST(2)}$ = 0.125). In the bio-neighbour-joining tree (Figure 4), E Spain-Sardinia-NE Morocco appeared as the basally branching group in the *Chamaerops* core, followed by France-Italy and, finally, by S Morocco and S Spain-N Morocco.

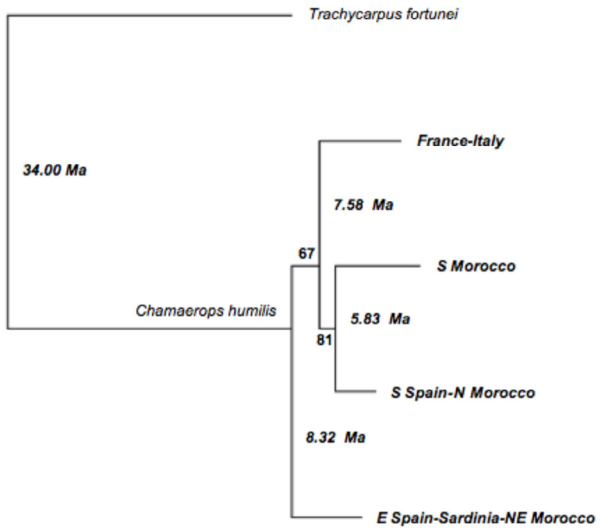

Figure 4. Bio-neighbour-joining tree for the Bayesian-inferred groups of populations (excluding NAPs) of *Chamaerops humilis* sampled, including *Trachycarpus fortunei* as an outgroup representative, based on the $\rho_{ST(2)}$ distances. Bootstrap values obtained on the chord distances for the neighbour-joining tree. Divergence times obtained from an AFLP-based molecular clock (Kropf et al., 2009).

Table 3. Results of the AMOVAs, considering different groupings and excluding not clearly assignable populations (NAPs: pops. 4, 16, and 18) according to Bayesian-inferred groups for K = 4. The best (lowest) Akaike and Schwarz criteria result is highlighted; see Section 2 for details.

	F_{CT} (95% CI)	Group % (d.f.)	Pop. % (d.f.)	Ind. % (d.f.)	*AIC*	*AICc*	*AICu*	*BIC*
No grouping	-	0.00 (0)	24.52 (18)	75.48 (171)	1377.31	4.44	4.45	752.98
var. *humilis* (pops. 1–18)/ var. *argentea* (pops. 19–22)	0.103 (0.079–0.130)	10.35 (1)	19.24 (17)	70.41 (171)	1367.42	4.40	4.41	746.48
N Mediterranean, islands included (pops. 1–13)/ S Mediterranean (pops. 14–22)	0.044 (0.031–0.057)	4.36 (1)	21.83 (17)	73.81 (171)	1370.99	4.41	4.43	750.05
Iberia (pops. 1–7)/France-Italy (pops. 8–9)/ Islands (pops. 10–13)/Morocco (pops. 14–22)	0.046 (0.033–0.060)	4.63 (3)	20.76 (15)	74.61 (171)	1365.05	4.39	4.41	750.90
Iberia (pops. 1–7)/France-Italy (pops. 8–9)/ Islands (pops. 10–13)/N Morocco (pops. 14–17)/ S Morocco (pops. 19–22)	0.072 (0.054–0.091)	7.19 (4)	18.31 (14)	74.50 (171)	1358.84	4.36	4.39	748.08
S Spain-N Morocco (pops. 1–3 and 14–15)/ E Spain-Sardinia-NE Morocco (pops. 5–7,10–11 and 17)/ France-Italy (pops. 8–9 and 12–13)/ S Morocco (pops. 19–22)	0.173 (0.150–0.196)	17.28 (3)	10.05 (15)	72.66 (171)	1343.77	4.29	4.31	729.62

3.4. Dating analysis

Plausible generation times arose when F_{IS} and rate values were the highest among those proposed, i.e. F_{IS} = 1 and 0.571 Ma/D_{N72}; smaller values resulted in higher generation times, of more than 1000 years at slow rates. When calibrating the first divergence between *T. fortunei* and *C. humilis* in the Late Eocene (at least 34 Ma), which resulted in a generation time of 309.45 years, the remaining nodes were then set to 8.32 Ma, 7.58 Ma, and 5.83 Ma for the E Spain-Sardinia-NE Morocco, France-Italy, and S Morocco and S Spain-N Morocco groups of populations respectively (Figure 4), i.e. in the Miocene.

3.5. Niche modelling

Results from niche modelling revealed a relatively narrow distribution of *C. humilis* during the last interglacial (Figure 5A), having been even narrower in the northern shore of the Mediterranean in the last glacial maximum (Figures 5B and 5C), although the degree of this narrowing was highly dependent on the atmospheric model chosen. The 4 groups of populations currently recognised also showed congruent distributional areas during this period. For the S Spain-N Morocco and the S Morocco groups, range alteration was not important (increasing even the potential range of this species in N Africa), but for the continental areas of the France-Italy and E Spain-Sardinia-NE Morocco groups, reduction might have been significant. For the islands sampled, there were extensions of suitable areas during the 3 time frames, and, remarkably, Corsica showed a very low likelihood of occurrence. There was probability of occurrence in Crete, as well as in some areas of Greece, Turkey, or the Levant, with the last ranges of suitable areas suffering minor alteration during the last glacial maximum (Figures 5A–5D).

4. Discussion

To infer the biogeographic processes that might explain the present distribution and patterns of genetic diversity among populations of *Chamaerops humilis*, several factors need to be taken into account. The phylogenetic context is important, because relationships to related genera might offer insights on location of origin. Likewise, fossil evidence is significant, because of the unusual morphology of this palm and relative abundance of dated fossil material. The historical climatic and geological changes in the West Mediterranean region, one of the most dynamic areas of the world, must also be taken into account. Finally, levels of genetic diversity within and among groups of populations as revealed in the phylogeographic analysis might suggest regions of ancestral refugia and/or recent migrations. These different sources of data, therefore, have been considered in the development of the biogeographic scenarios presented herein.

4.1. Outgroup relationships and fossil evidence

To infer the ancient distribution of *Chamaerops humilis*, it is helpful to understand the phylogenetic relationships between it and close generic relatives. *Chamaerops* belongs

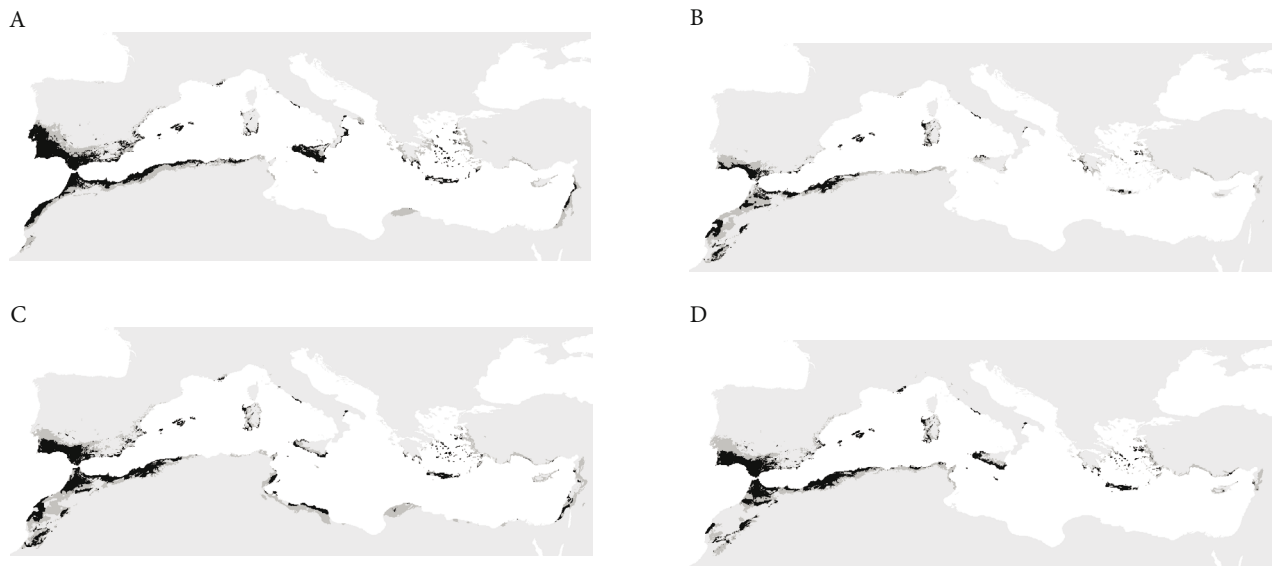

Figure 5. Suitable areas for *Chamaerops humilis* estimated in 3 periods: last interglacial (LIG, ~120,000–140,000 years BP; **A**); last glacial maximum (LGM, ~21,000 years BP), **B** for CCSM and **C** for MIROC atmospheric models; and present period (**D**, ~1950–2000). Results shown were obtained from niche modelling analyses considering both bioclim and soil data, for 2 thresholds: maximum training sensitivity plus specificity logistic threshold (in dark grey) and 10-percentile training presence logistic threshold (in black). LIG and LGM are represented with current coastlines.

to subfamily Coryphoideae of Palmae (Arecaceae). According to the classification by Asmussen et al. (2006), based on several plastid DNA regions, this subfamily with approximately 45 genera has been divided into 3 major clades (also supported by Baker et al., 2009). The first clade consists entirely of New World taxa, the second clade consists mainly of Old World taxa, and the second is sister to the third clade containing only the Old World genus *Phoenix*. *Chamaerops humilis* occurs in the second clade and is sister to other taxa from Asia (mainly in China and the Malayan Peninsula), such as *Trachycarpus fortunei*; *Guihaia argyrata* (S.K.Lee & F.N.Wei) S.K.Lee, F.N.Wei & J.Dransfield; *Rhapis excelsa* (Thunb.) A.Henry; and *Maxburretia rupicola* (Ridl.) Furtado. *Rhapidophyllum hystrix* (Pursh) H.Wendl. & Drude is the lone New World species also in this clade. Some of these taxa were, in fact, considered as *Chamaerops* species in the past (see Govaerts and Dransfield, 2005). Phylogenetic evidence, therefore, points more strongly to the possibility that *Chamaerops* originated in the Old World rather than the New World.

Fossil evidence reveals that *Chamaerops* was an important element of the European flora at least since the Eocene and further reinforces this region as being ancestral for the genus.

4.2. Changes in the Mediterranean region

To understand the biogeography of *Chamaerops* also necessitates examination of geological and climatic changes that have taken place in the West Mediterranean region during the past 30 Ma. The northern and the southern shores of this sea have remained separate or have been linked via land bridges, such as occurred during the Messinian salinity crisis (6.0–5.3 Ma) when water flow from the Atlantic Ocean was dramatically reduced (Duggen et al., 2003; García-Castellanos and Villaseñor, 2011). Climate also changed from a paratropical environment in the Eocene to a Mediterranean-like climate in the Pliocene (Mai, 1989; Carrión, 2003; Thompson, 2005). These inferences support the idea of a suitable environment in the West Mediterranean region for *Chamaerops* during the Oligocene-Miocene time.

We can infer that the influence of Quaternary glaciations led to a reduction of the area of distribution of *Chamaerops* in most areas of the northern shore of the Mediterranean. For the last glacial maximum, assessment of the degree of this reduction depends upon the atmospheric model chosen (Figures 5B and 5C). The MIROC model (Figure 5C) seems less probable than the CCSM model, because the species distribution it generates for a much cooler period is too similar to that of the present. Interestingly, the species occurrence in Crete, which was predicted by the niche modelling analyses, has also been confirmed by historical records (Médail and Quézel, 1996). Fluctuating glaciations in the Pleistocene brought winter snow to most of the northern territories (Carrión, 2003; Thompson, 2005). It is during this period that the Mediterranean Basin served as a refugium for some genera such as *Abies* (Terrab et al., 2007), among others.

4.3. Phylogeographic structure among populations

Chamaerops humilis population structure as shown by Bayesian inference, Neighbour-Net graph (supported by the bootstrap values), PCoAs, and AMOVAs reveals the existence of 4 groups of populations (Tables 2 and 3; Figures 1–3).

Genetic diversity within populations helps clarify some of the relationships observed. The France-Italy group exhibits, globally, the lowest percentage of polymorphism and genetic diversity, but one of the highest values of rare fragments index calculated for the group as a whole (equal to the S Morocco group). The E Spain-Sardinia-NE Morocco group shows the highest level of polymorphism and genetic diversity, but the lowest value of rare fragments index (see Table 4), which, together with the NJ tree and the dating analysis, suggests this as a possible ancestral

Table 4. Bayesian-inferred groups of populations. Sample size (n), $Frag_{tot}$, $Frag_{poly}$ (%), number of phenotypes (n_{ph}), H_D (mean and SE), and *DW* (calculated for the groups as a whole) are shown. Nonassignable populations, according to Bayesian-inferred groups for $K = 4$, are not included (NAPs: pops. 4, 16, and 18).

Group of populations	n	$Frag_{tot}$	$Frag_{poly}$ (%)	n_{ph}	H_D (SE)	*DW*
E Spain-Sardinia-NE Morocco (pops. 5–7, 10–11, and 17)	60	185	166 (89.7%)	56	0.281 (0.013)	230.7
France-Italy (pops. 8–9 and 12–13)	40	186	154 (82.8%)	40	0.258 (0.013)	281.1
S Spain-N Morocco (pops. 1–3 and 14–15)	50	185	156 (84.3%)	50	0.265 (0.012)	262.9
S Morocco (pops. 19–22)	40	186	156 (83.9%)	37	0.262 (0.012)	296.9
Chamaerops humilis	190	206	198 (96.1%)	183		
Trachycarpus fortunei	10	106	61 (57.5%)	8		

group of populations. The differences among the 4 regions, however, are not large, although those populations with the lowest diversity are located in the France-Italy group (Circeo and Syracuse) and in the S Morocco group (Beni Mellal). Two populations between well-defined units, i.e. Tarifa and Tazzeka, showed a higher diversity index, possibly as a result of recent secondary contact (Table 1; Figures 2 and 6). It is also interesting that separation among populations within each of the groups is small, as can be seen in the PCoA and in the AMOVAs (Table 3). That result might be explained by long generation times, which dampen differentiation through slow turnover of populations. Individuals of *Chamaerops humilis* can survive for several centuries, as has been observed in European gardens during the past 400 years (del Cañizo, 2011).

According to the divergence values, one can determine the relative ages of the genetic groups of populations within *Chamaerops humilis*. Based on the bio-neighbour-joining tree (Figure 4), calculated with the pairwise $\rho_{ST(2)}$ values, the E Spain-Sardinia-NE Morocco group of populations appears to be slightly older, as it is the group closest to the outgroup representative, *Trachycarpus fortunei*, a species currently restricted to China (del Cañizo, 2011).

4.4. Biogeography

Based on generic relationships, fossil evidence, geological and climatic changes in the Mediterranean region, and population genetic variation, a biogeographical scenario can be formulated to explain the present distribution of *Chamaerops humilis*. Additional factors also need to be taken into account, however, such as the biological dispersal potentials of *C. humilis*, the existing geographical barriers to dispersal in the region, and age estimates from the AFLP-based molecular clock.

Biological characteristics of *Chamaerops humilis* provide limits to its dispersal potentials. In this species, pollen can travel with the help of weevils or, less likely, by wind (Herrera, 1989; Düffay and Astett, 2004), but very long distances are not usually traversed (Carrión, 2002). Bird seed dispersal, as suggested by Terrab et al. (2008) for *Juniperus thurifera* in relation to the Corsican-Sardinian microplate, is not plausible for fruits of *C. humilis*, as the fruits are mammal-dispersed (Fedriani and Delibes, 2011; JL García-Castaño, unpubl. res.). Seeds might occasionally be carried by the sea, although fresh seeds do not float well in normal seawater. Degraded fruit pulp with associated seeds could, however, due to air chambers, successfully traverse some distance (JL García-Castaño, unpubl. res.), but germination after such immersions has not yet been tested.

Humans, therefore, are the most likely overseas dispersers of *Chamaerops humilis*, and this during historical time (directly or indirectly, for example by goats; JL García-Castaño, unpubl. res.). *Chamaerops humilis* has been used traditionally for food (fruits, young flowers, young leaf petioles, and rhizome meristems), and for making brooms and handicrafts from its fibrous leaves, but it seems that there has been no large-scale commerce with seeds or trunks (see Gaius Plinius Secundus, Pliny the Elder, 1st century AD; del Cañizo, 2011), as has been considered for the more economically important *Olea* (Terral et al., 2004). Commercial sales of *C. humilis* as a garden plant, however, have been increasing during the past century (cf. numerous web pages).

Some natural geographical barriers to dispersal of *C. humilis* also exist. Barriers isolating E Spain from the France-Italy populations reflect climatic or soil characteristics of the intervening zone, as the niche modelling analyses have shown. The border between populations in France-Italy and N Africa might also be maintained by the Mediterranean Sea. The Tunisian and Algerian populations were not studied, however, and some authors have found a similarity between S Italy and Tunisia populations in other species (see Ortiz et al., 2009). Separation between the S Spain-N Morocco and S Morocco (var. *argentea*, at higher altitudes) populations might have been promoted by habitat differences (the bluish cast of the leaves is a not uncommon phenomenon in alpine plants to protect against excessive UV radiation; Körner, 2003).

The estimation obtained with the AFLP-based molecular clock for divergences within *C. humilis* points to a relatively old time frame of 5.83–8.32 Ma, in the Miocene (Figure 4). Because of problems associated with this type of dating analysis (Ehrich et al., 2009), these estimates must be regarded as tentative, but they do at least suggest an origin before the Pleistocene (2.59–0.01 Ma) and are congruent with the 6.20 Ma (95% CI: 2.34–10.57 Ma) for *Chamaerops* at its crown node as reported by Bacon et al. (2012).

Taking all aspects into consideration, we integrate several biogeographic divergence events into a comprehensive scenario. The first event would have taken place in the Gulf of Lyon, separating the E Iberian and the Italian populations due to lack of intermixing as a consequence of long distance separating both regions. From these Italian populations, expansion would have occurred to Africa through the area that eventually became Sicily (connected to the Italian Peninsula and Africa in the Oligocene and in the Miocene) and Tunisia, and populations may have extended more or less continuously along or near the coast (Figure 6). Second, this expansion reached 2 final destinations, southward, to the High Atlas and beyond, and westward and northward, crossing finally to the former Iberian Peninsula via the land bridge that existed in the Messinian salinity crisis (6.0–5.3 Ma) in the current Strait of Gibraltar (Duggen et al., 2003; García-

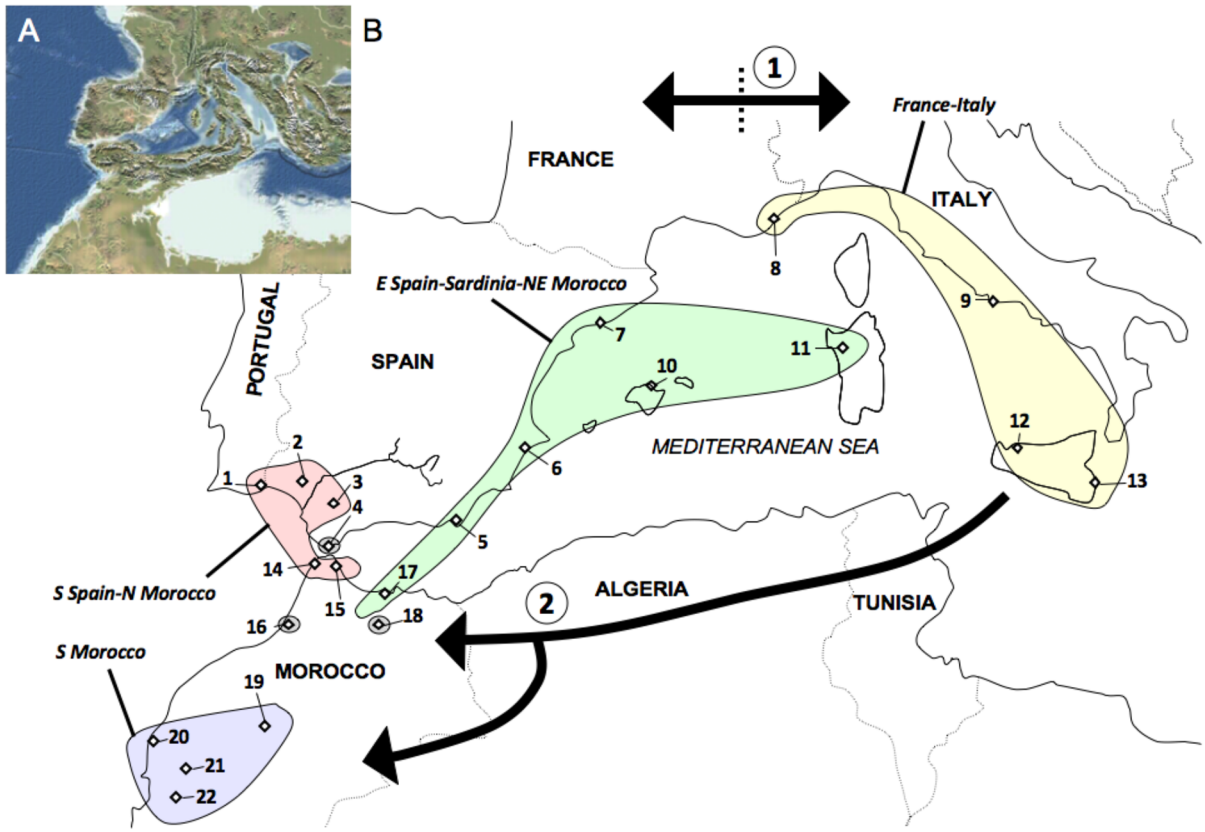

Figure 6. Maps of **(A)** the West Mediterranean emerged lands at Late Oligocene–Early Miocene and **(B)** population allocations to the Bayesian-inferred groups of populations and the 2 main bifurcations of the expansion routes (in grey, NAPs: pops. 4, 16, and 18); see Table 1 for codes. Inset palaeomap modified and reproduced with the permission of Ron Blakey, Northern Arizona University.

Castellanos and Villaseñor, 2011). Populations might have also been able to cross the Strait of Gibraltar, aided by lower sea levels during the Pleistocene that would have produced small islands as stepping-stones. This recent connection has been hypothesised for other taxa, such as *Hypochaeris* (Ortiz et al., 2009), among others. These 2 expansionary lineages, i.e. S-Spain-N Morocco and S Morocco, would then have remained isolated for long periods of time due to a water barrier between them, which began to disappear at the Miocene-Pliocene boundary and which was covered by sediments during the Quaternary (Zouhri et al., 2001). This allowed secondary contact between population systems and genetic intermixing in the Mamora region (see Ortiz et al., 2009). Third, another expansion of *Chamaerops* resulted in a peculiar distributional pattern at a more regional scale. Populations from E Spain, the Balearics, and Al Hoceima may have all appeared as a result of microplate migrations from the Oligocene onwards that gave rise to the large islands of the northern Mediterranean as well as land areas joined to the North African mainland (Magri et al., 2007) or, more recently, during the Messinian salinity crisis (Duggen et al., 2003; Meijer and Krijgsman, 2005; García-Castellanos and Villaseñor, 2011). The last option seems to be more likely due to the high similarity of these populations.

Traces of a past expansion dating from the Tertiary have also been recorded in other Mediterranean species such as *Erophaca baetica* (Casimiro-Soriguer et al., 2010), through a E-W vicariance or *Quercus suber* (Magri et al., 2007), with a similar pattern to the one reported here. Effects of glaciations have also been documented for genera such as *Abies* (Terrab et al., 2007) or *Juniperus* (Terrab et al., 2008).

It is also possible to consider other biogeographic explanations for the present distribution of *C. humilis* in the West Mediterranean. Populations might have moved in the Tertiary to Italy via West Mediterranean microplate migration, as some of them could have joined with the newly formed Italian Peninsula, with subsequent changes as outlined above (see Rosenbaum et al., 2002). Another possibility during the Tertiary might be through a 'counter-clockwise' route from E Spain to S Spain-N Morocco, and from here first to France-Italy and later to S Morocco. Of these 2 alternatives, the first alternative is plausible, as

formation of the Alps might have made access to the new Italian Peninsula difficult (Rosenbaum et al., 2002). The second alternative, however, would require an overseas connection (Duggen et al., 2003; García-Castellanos and Villaseñor, 2011), which we also regard as unlikely. The lack of fossils from N Africa does not help support any particular hypothesis.

4.5. Implications for taxonomy and conservation

Conservation of *Chamaerops humilis*, a plant unusual within the Mediterranean landscape and an unusual palm worldwide, should be focused not only on the species itself (it is, for example, protected by regional environmental law as of 1997 in Andalusia, Spain), but more precisely on each of the 2 recognised varieties. Variety *argentea* is morphologically the most divergent group of populations (with a bluish or pruinose cast), but these are not particularly divergent genetically. One could also make a strong argument, however, for conservation of each of the 4 genetic groups of populations revealed in the present study. They are sufficiently genetically distinct to warrant priority of conserving at least some populations within each of these disparate geographic regions.

4.6. Summary

The present population structure found in *Chamaerops humilis* can be explained best by considering patterns of expansion to a more or less wide distribution and posterior vicariance in the West Mediterranean region. The current distribution of populations of this species seems to have been influenced by its ancient area in continental Europe, by plate tectonic movements over long periods of geological time, and by reduction and shifting of populations during the colder Quaternary.

Acknowledgements

We thank Juan García, Elisa Castaño, María del Carmen García, María del Carmen Crespo, Jesús del Gran Poder Rodríguez-Sánchez, Francisca Godino, Daniel Sánchez, Susana Godino, Marie-Charlotte Anstett, Juan Luis García-Mudarra, Stefania Pissanu, Pedro Jesús Gea, Sergio Braña, Mercedes Domínguez, Alberto García (Alamillo nursery, Seville, Spain), Modesto Luceño, and Eduardo Narbona, for help with field collections; Rosabelle Samuel, Michael HJ Barfuss, Elfriede Grasserbauer, Verena Klejna, and, very specially, Gudrun Kohl, for help with laboratory work; Jose Manuel Sánchez-Robles for providing useful suggestions; and research grants from the Ministerio de Educación y Ciencia to Montserrat Arista (CGL2005-01951, Spain) and the Secretaría General de Universidades, Investigación y Tecnología (Convocatoria 1/2006, Junta de Andalucía, Spain) to JLG-C.

References

Akaike H (1974). A new look at the statistical model identification. IEEE T Automat Contr 19: 716–723.

Applied Biosystems (1989–2000). GeneScan version 3.1.2. Foster City, CA, USA: Applied Biosystems.

Asmussen CB, Dransfield J, Deickmann V, Barfod AS, Pintaud JC, Baker WJ (2006). A new subfamily classification of the palm family (Arecaceae): evidence from plastid DNA phylogeny. Bot J Linnean Soc 151: 15–38.

Avise JC (2000). Phylogeography: The History and Formation of Species. Cambridge, MA, USA: Harvard University Press.

Bacon CD, Baker WJ, Simmons MP (2012). Miocene dispersal drives island radiations in the palm tribe Trachycarpeae (Arecaceae). Syst Biol 61: 426–442.

Baker WJ, Savolainen V, Asmussen-Lange CB, Chase MW, Dransfield J, Forest F, Harley MM, Uh NW, Wilkinson M (2009). Complete generic-level phylogenetic analyses of palms (Arecaceae) with comparisons of supertree and supermatrix approaches. Syst Biol 58: 240–256.

Benham J, Jeung JU, Jasieniuk M, Kanazin V, Blake T (1999). Genographer: a graphical tool for automated fluorescent AFLP and microsatellite analysis. J Agric Genomics 4: 3.

Blears MJ, De Grandis SA, Lee H, Trevors JT (1998). Amplified fragment length polymorphism (AFLP): a review of the procedure and its applications. J Ind Microbiol Biot 21: 99–114.

Bonin A, Ehrich D, Manel S (2007). Statistical analysis of amplified fragment length polymorphism data: a toolbox for molecular ecologists and evolutionists. Mol Ecol 16: 3737–3758.

Braconnot P, Otto-Bliesner B, Harrison S, Joussaume S, Peterschmitt JY, Abe-Ouchi A, Crucifix M, Driesschaert E, Fichefet T, Hewitt CD et al. (2007). Results of PMIP2 coupled simulations of the Mid-Holocene and Last Glacial Maximum - Part 1: experiments and large-scale features. Clim Past 3: 261–277.

Carrión JS (2002). A taphonomic study of modern pollen assemblages from dung and surface sediments in arid environments of Spain. Rev Palaeobot Palyno 120: 217–232.

Carrión JS (2003). Evolución vegetal. Murcia, Spain: Diego Marín Librero-Editor (in Spanish).

Carrión JS, editor (2012). Paleoflora y paleovegetación de la Península Ibérica e Islas Baleares: Plioceno–Cuaternario. Madrid, Spain: Ministerio de Economía y Competitividad (in Spanish).

Casimiro-Soriguer R, Talavera M, Balao F, Terrab A, Herrera J, Talavera S (2010). Phylogeny and genetic structure of *Erophaca* (Leguminosae), a East-West Mediterranean disjunct genus from the Tertiary. Mol Phylog Evol 56: 441–450.

del Cañizo JA (2011). Palmeras. 3rd ed. Madrid, Spain: Ediciones Mundi-Prensa (in Spanish).

do Amaral Franco J (1980) *Chamaerops*. In: Tutin TG, Heywood VH, Burges NA, Moore DM, Valentine DH, Walters SM, Webb DA, editors. *Flora Europaea*, Vol. V. Cambridge, UK: Cambridge University Press, p. 267.

Doyle JJ, Doyle JL (1987). A rapid DNA isolation procedure from small quantities of fresh leaf tissues. Phytochem Bull 19: 11–15.

Dransfield J, Uhl NW, Asmussen CB, Baker WJ, Harley MM, Lewis CE (2008). *Genera Palmarum*. Evolution and Classification of the Palms. 2nd ed. London, UK: Royal Botanic Gardens, pp. 247–249.

Düfay M., Anstett MC (2004). Cheating is not always punished: killer female plants and pollination by deceit in the dwarf palm *Chamaerops humilis*. J Evolution Biol 17: 862–868.

Duggen S, Hoernle K, van den Bogaard P, Rüpke L, Morgan JP (2003). Deep roots of the Messinian salinity crisis. Nature 422: 602–606.

Ehrich D (2006). AFLPdat: a collection of R functions for convenient handling of AFLP data. Mol Ecol Notes 6: 603–604.

Ehrich D, Eidesen PB, Alsos IG, Brochmannm C (2009). An AFLP clock for absolute dating of shallow-time evolutionary history – too good to be true? Mol Ecol 18: 4526–4532.

El Mousadik A, Petit RJ (1996). High level of genetic differentiation for allelic richness among populations of the argan tree [*Argania spinosa* (L.) Skeels] endemic to Morocco. Theor Appl Genet 92: 832–839.

Excoffier L, Laval G, Schneider S (2005). Arlequin version 3.0: an integrated software package for population genetics data analysis. Evol Bioinform Online 1: 47–50.

Falush D, Stephens M, Pritchard JK (2003). Inference of population structure using multilocus genotype data: linked loci and correlated allele frequencies. Genetics 164: 1567–1587.

FAO/IIASA/ISRIC/ISSCAS/JRC (2012). Harmonized World Soil Database (version 1.2). Rome, Italy: FAO, and Laxenburg, Austria: IIASA.

Fedriani JM, Delibes M (2011). Dangerous liaisons disperse the Mediterranean dwarf palm: fleshy-pulp defensive role against seed predators. Ecology 92: 304–315.

García-Castellanos D, Villaseñor A (2011). Messinian salinity crisis regulated by competing tectonics and erosion at the Gibraltar Arc. Nature 480: 359–363.

Givulescu R, Barbu O (1999). Eine fossile Palme *Chamaerops humilis* Linné fossilis Kolakovski aus dem Miozän von Rumänien. Beiträge zur Paläontologie 24: 87–90 (in German).

Govaerts R, Dransfield J (2005). World Checklist of Palms. London, UK: The Board of Trustees of the Royal Botanic Gardens, Kew Publishing.

Herrera CM (1995). Plant-vertebrate seed dispersal systems in the Mediterranean: ecological, evolutionary, and historical determinants. Annu Rev Ecol Syst 26: 705–727.

Herrera J (1989). On the reproductive biology of the dwarf palm, *Chamaerops humilis* in Southern Spain. Principes 33: 27–32.

Hijmans RJ, Cameron SE, Parra JL, Jones PG, Jarvis A (2005). Very high resolution interpolated climate surfaces for global land areas. Int J Climatol 25: 1965–1978.

Huson DH, Bryant D (2006). Application of phylogenetic networks in evolutionary studies. Mol Biol Evol 23: 254–267.

Jafri SMH, El-Gadi A (1977). Flora of Libya, Vol. XXXVI. Tripoli, Libya: Al-Faateh University.

Jakobsson M, Rosenberg NA (2007). CLUMPP: a cluster matching and permutation program for dealing with label switching and multimodality in analysis of population structure. Bioinformatics 23: 1801–1806.

Körner C (2003). Alpine Plant Life: Functional Plant Ecology of High Mountain Ecosystems. 2nd ed. Berlin, Germany: Springer Verlag.

Kovar-Eder J, Kvaček Z, Martinetto E, Roiron P (2006). Late Miocene to Early Pliocene vegetation of Southern Europe (7–4 Ma) as reflected in the megafossil plant record. Palaeogeogr Palaeocl 238: 321–339.

Kropf M, Comes HP, Kadereit JW (2009). An AFLP clock for the absolute dating of shallow-time evolutionary history based on the intraspecific divergence of southwestern European alpine plant species. Mol Ecol 18: 697–708.

Magri D, Fineschi S, Bellarosa R, Buonamici A, Sebastiani F, Schirone B, Simeone MC, Vendramin GG (2007). The distribution of *Quercus suber* chloroplast haplotypes matches the palaeographical history of the Western Mediterranean. Mol Ecol 16: 5259–5266.

Mai DH (1989). Development and regional differentiation of the European vegetation during the Tertiary. Plant Syst Evol 162: 79–91.

Maire R (1980). Flore de L'Afrique du Nord, Vol. XV. Paris, France: L'Imprimerie Jouve pour les Éditions Lechevalier S.A.R.L. (in French).

McQuarrie ADR, Tsai CL (1998). Regression and Time Series Model Selection. Singapore: World Scientific Publishing.

Médail F, Quézel P (1996). Signification climatique et phyto-écologique de la redécouverte en France méditerranéenne de *Chamaerops humilis* L. (Palmae). Comptes rendus de l'Académie des sciences (Paris), Sciences de la vie 319: 139–45 (in French).

Meijer PTh, Krijgsman W (2005). A quantitative analysis of the desiccation and re-filling of the Mediterranean during the Messinian Salinity Crisis. Earth Planet Sc Lett 240: 510–520.

Ortiz MÁ, Tremetsberger K, Stuessy T, Terrab A, García-Castaño JL, Talavera S (2009). Phylogeographic patterns in *Hypochaeris* section *Hypochaeris* (Asteraceae, Lactuceae) of the Western Mediterranean. J Biogeogr 36: 1384–1397.

Otto-Bliesner BL, Marshall SJ, Overpeck JT, Miller GH, Hu A (2006) Simulating Arctic climate warmth and icefield retreat in the last interglaciation. Science 311: 1751–1753.

Palamarev E (1989). Paleobotanical evidences of the Tertiary history and origin of the Mediterranean sclerophyll dendroflora. Plant Syst Evol 162: 93–107.

Palamarev E, Bozukov V, Uzunova K, Petkova A, Kitanov G (2005). Catalogue of the Cenozoic plants of Bulgaria (Eocene to Pliocene). Phytologia Balcanica 11: 215–364.

Phillips SJ, Anderson RP, Schapire RE (2006). Maximum entropy modeling of species geographic distributions. Ecol Model 190: 231–259.

Plinius Secundus G (1st century AD). *Naturalis Historiae*, Vol. XIII. In: Bostock J, Riley HT, translators (1855). The Natural History of Pliny, Vol. III. London, UK: HG Bohn.

Pons A (1981). The history of the Mediterranean shrublands. In: di Castri F, Goodall DW, Specht RL, editors. Mediterranean-Type Shrublands. Amsterdam, the Netherlands: Elsevier Science Publishing Company, p. 131–138.

Pritchard JM, Stephens M, Donnelly P (2000). Inference of population structure from multilocus genotype data. Genetics 155: 945–959.

Rosenbaum G, Lister GS, Duboz C (2002). Reconstruction of the tectonic evolution of the Western Mediterranean since the Oligocene. In: Rosenbaum G, Lister GS, editors. Reconstruction of the Evolution of the Alpine-Himalayan Orogen. Journal of the Virtual Explorer 8: 107–130.

Rosenberg NA (2004). Distruct: a program for the graphical display of population structure. Mol Ecol Notes 4: 137–138.

Schlüter PM, Harris SA (2006). Analysis of multilocus fingerprinting data sets containing missing data. Mol Ecol Notes 6: 569–572.

Schwarz G (1978). Estimating the dimension of a model. Ann Stat 6: 461–464.

Skrede I, Bronken Eidesen P, Piñeiro Portela R, Brochmann C (2006). Refugia, differentiation and postglacial migration in arcticalpine Eurasia, exemplified by the mountain avens (*Dryas octopetala* L.). Mol Ecol 15: 1827–1840.

Terrab A, Schönswetter P, Talavera S, Vela E, Stuessy TF (2008). Range-wide phylogeography of *Juniperus thurifera* L., a presumptive keystone species of Western Mediterranean vegetation during cold stages of the Pleistocene. Mol Phylogenet Evol 48: 94–102.

Terrab A, Talavera S, Arista M, Paun O, Stuessy TF, Tremetsberger K (2007). Genetic diversity and geographic structure at chloroplast microsatellites (cpSSRs) in endangered West Mediterranean firs (*Abies* spp., Pinaceae). Taxon 56: 409–416.

Terral JF, Alonso N, Capdevila RBI, Chatti N, Fabre L, Fiorentino G, Marinval P, Jordá GP, Pradat B, Rovira N et al. (2004). Historical biogeography of olive domestication (*Olea europaea* L.) as revealed by geometrical morphometry applied to biological and archaeological material. J Biogeogr 31: 63–77.

Thompson JD (2005). Plant Evolution in the Mediterranean. New York, NY, USA: Oxford University Press.

Velitzelos E, Gregor HJ (1990). Some aspects of the Neogene floral history in Greece. Rev Palaeobot Palyno 62: 291–307.

Vos P, Hogers R, Bleeker M, Reijans M, van de Lee T, Homes M, Frijters A, Pot J, Peleman J, Kuiper M et al. (1995). AFLP: a new technique for DNA fingerprinting. Nucleic Acids Res 23: 4407–4414.

Yeh FC, Boyle TJB (1997). Population genetic analysis of co-dominant and dominant markers and quantitative traits. Belg J Bot 129: 157.

Zouhri L, Lamouroux C, Buret C (2001). The Mamora Plain, a hinge between the Meseta and the Rif. Its importance in the post-Paleozoic geodynamic evolution of Morocco. Geodin Acta 14: 361–372.

Supplementary material

Figure S1. *Chamaerops humilis* individual in a typical Mediterranean *Quercus* L. forest from pop. 3 (Pruna, Spain).